

1.3.5. Preliminary Induced Seismicity Mitigation Plan.

This is a preliminary plan following the protocol established by Majer et al. (2012). Information that was collected in Phase 1 has been incorporated, as has initial literature searches and preliminary risk assessments. This document will be updated and finalized in Phase 2C.

1. Preliminary Screening Evaluation

The Utah FORGE site is located in the West Desert of Utah in Beaver County. This is a rural area. The nearest population center is the town of Milford, located 16 km away. Milford has a population of ~1400. Critical facilities include a hospital, an airport and schools. Other facilities in the vicinity of the Utah FORGE site include a geothermal plant, wind farm, solar facility, transmission line and natural gas pipeline. Based on 2010 Census Bureau data, there are ~2500 households and a total population of 6,629 in Beaver County, with the majority of the population located in the town of Beaver, 32 km southeast of the deep drill site. The majority of the built environment is residential. Based on the population and the built environment, the preliminary assessment is that this is a low seismic risk area.

In regards to hazard, the University of Utah Seismograph Stations (UUSS) has been monitoring seismic activity in Utah and the surrounding region for the past 50 years and has compiled an earthquake catalog going back to 1850 (Figure 1). Based on this historical record, there has been only one $M > 4$ earthquake in the greater Milford, FORGE study area. This was the 1908 M 4.08 Milford earthquake located south of the town. Within ~50km of the Utah FORGE site, there have been other earthquakes $M > 4.0$ but only one earthquake $M \geq 5.0$, the 1901 M 6.6 Tushar Mountain earthquake (#2, Figure 1) located >50 km to the east. Based on both the UUSS catalog and an early study by Zandt et al. (1982), the Utah FORGE study area is characterized by small magnitude earthquakes and a low seismic rate. A more complete analysis of the seismicity is presented in section 5.

The 2008 U.S. Geological Survey National Seismic Hazard Maps (Peterson et al., 2008) shows the Utah FORGE study area to be in a region of low- to moderate-seismic hazard (Figure 2). There is a 0.2 to 0.25 probability of an $M > 5$ earthquake within 50 km in the next 20 years, and there is a 10% probability that the peak ground acceleration (PGA) will exceed 10% g in the next 50 years. Deaggregation shows that the largest contribution to the PGA 10% in 50 years hazard comes from $M < 6.5$ earthquakes within 25 km of the site. More information regarding hazard and risk can be found in Sections 5 and 6.

In addition to the earthquake hazard, there are other known seismic sources in the area. There is a large quarry operation northwest of Milford producing seismic events of similar magnitude ($M < 2$) and ground motions to the majority of cataloged earthquakes. Additionally, there is the possibility of small ground motions associated with railway traffic through the town of Milford, and noise sources related to the railroad and air traffic. To our knowledge, there are no state or local regulations related to induced seismicity. In regard to ground motions, the state has adopted the International Building Codes.

Based on: (1) the rural nature (low risk) of the proposed site; (2) that the expected EGS seismicity will be smaller or equal in magnitude to the background tectonic hazard; and (3) the

on-going nuisance ground motion and noise related to the quarry, railway, and airport, our *preliminary* analysis classifies the overall risk as very low (I) to low (II).

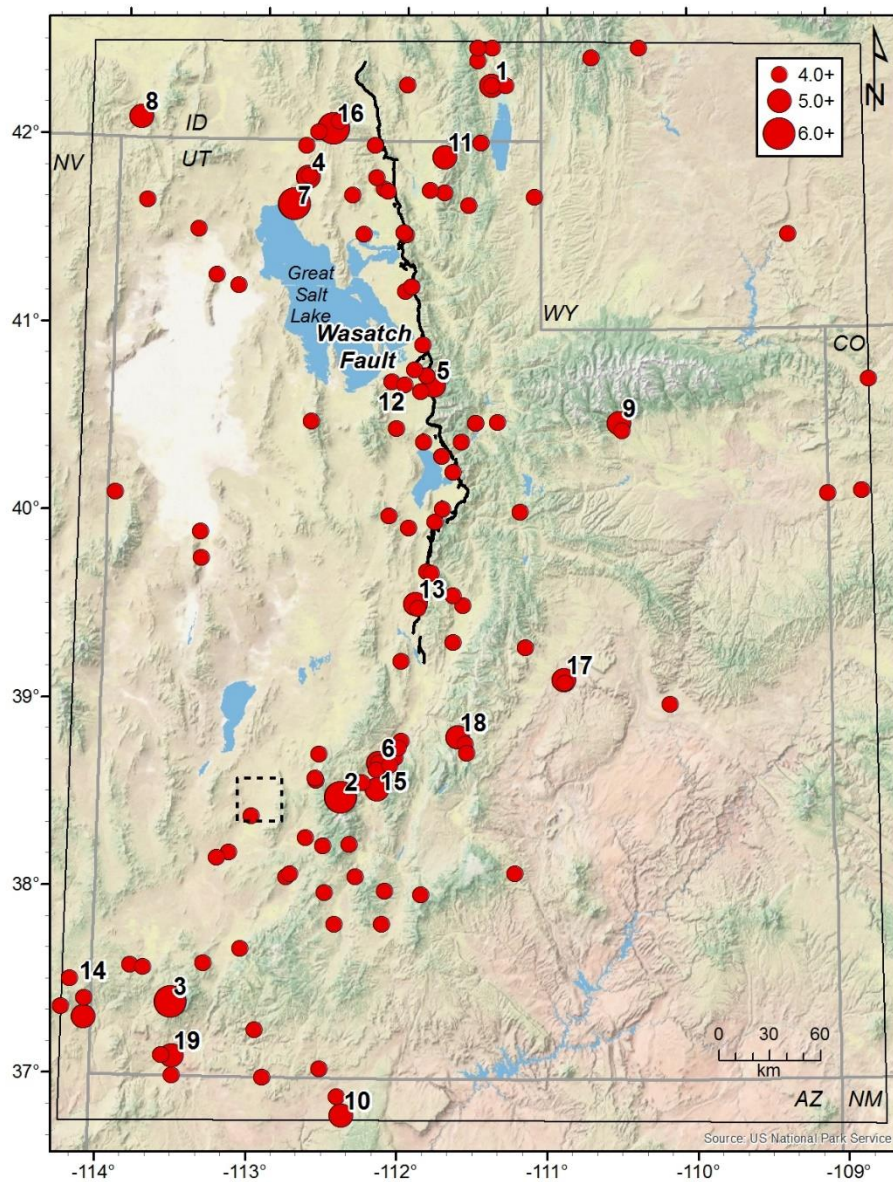


Figure 1. Epicenter map of main shocks of moment magnitude, $M > 4.0$ in the Utah Region, 1850 through September 2012; foreshocks, aftershocks, and mining-related seismicity are excluded. Data are from a revision of Utah's historical earthquake catalog (Arabasz et al., 2015).

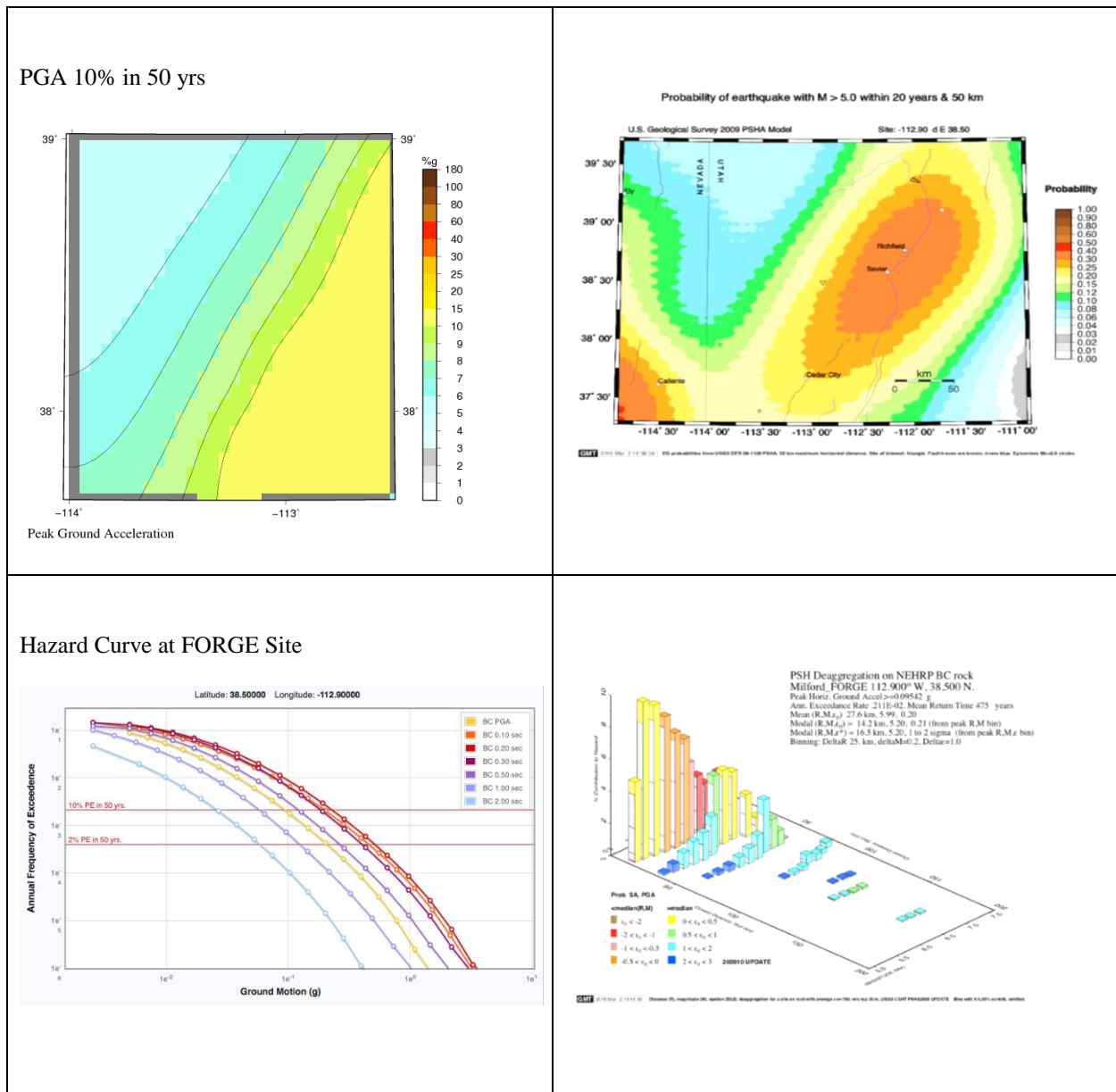


Figure 2. Probabilistic seismic hazard at the FORGE site from the 2008 National Seismic Hazard map and tools found at (<http://earthquake.usgs.gov/hazards/apps/>; last accessed 3/2/2016). (a) PGA with a 10% probability of exceedance in 50 yrs is 10%g at the site. (b) The probability of an $M > 5.0$ earthquake within 50 km of the FORGE site in the next 20 years is 0.20 to 0.25. (c) Hazard curves for the FORGE site for selected frequencies (PGA to 0.5 Hz). (d) Deaggregation for the 10% in 50 yrs PGA hazard (475 yr return period). Results show that the largest contribution to this hazard is from $M 5.2$ earthquakes at 14 km distance.

2. Outreach and Communication Program

A comprehensive and detailed description of Utah FORGE communication and outreach protocol and activities is provided in the Communications and Outreach Plan of this report. The following covers activities and approaches relevant and specific to seismic mitigation.

Although the Utah FORGE site is believed to be in a low seismic risk area, the project offers an opportunity to inform and educate the general public and other stakeholders about seismic monitoring methods, ground vibration and seismic noise, and the hazards of natural and induced seismic events both in the project area and beyond.

Stakeholders

Utah FORGE is located within the Milford renewable energy corridor that is host to two geothermal plants, a solar and wind farm, a biogas facility, and several major transmission lines. In addition to energy corridor stakeholders, seismic mitigation communication and outreach efforts will target residents, business, and government organizations in Milford, and elsewhere in Beaver County, Utah. See the Communications and Outreach Plan (Task 1.3.4) for a complete list of Utah FORGE stakeholders.

Seismic Mitigation Communications and Outreach Contacts

All participants in the Utah FORGE project are expected to contribute to communications and outreach activities as requested by the project management team (PMT) or the DOE. Dr. Joseph Moore, Managing Principal Investigator (PI), will oversee communication and outreach activities and serve as the contact point with the DOE. For seismic mitigation activities, the PI will be supported by Dr. Kristine Pankow, Associate Director, University of Utah Seismograph Stations; Mr. Lance Weaver, Utah Forge Website Administrator; and Mr. Mark Milligan, Utah FORGE Outreach Coordinator and main point of contact for public outreach activities. Emergency contact information is provided at the end of this section.

Dr. Kristine Pankow will conduct seismic monitoring and mitigation activities for the Utah FORGE project. The website administrator will manage the website, working closely with the outreach coordinator to include current information on seismic mitigation. The outreach coordinator will seek out opportunities to highlight activities related to seismic mitigation on the Utah FORGE project. He will serve as a primary contact with the public and will work closely with the website administrator.

Seismic Mitigation Communications Activities and Protocols

Good communications are essential to avoid misconceptions by the general public and other stakeholders about the hazard and resultant risk, regardless of how low, associated with Utah FORGE activities. As operations proceed, Utah FORGE will apprise stakeholders and seek feedback. To maintain transparency, promote education, and foster a continued rapport with stakeholders, Utah FORGE will conduct and adhere to the following activities and protocols:

- a. Hold stakeholder meetings prior to any activities that may produce or be perceived to produce ground vibration, seismic noise, or induced seismicity. At minimum, we will hold an initial public meeting that covers technical and non-technical issues, and hold additional meetings in advance of the first stimulation and after the stimulation to report

on the results. We will notify stakeholders of these meetings and advertise them to the general public in Milford and the rest of Beaver County. Additional meetings will be conducted as appropriate.

- b. Conduct stakeholder site visits annually, with additional visits during active drilling and stimulation.
- c. Install a display for real-time seismic monitoring in the Utah FORGE site office.
- d. Install an outreach display including a monitor for real-time seismic data in the Milford High School library, pending final approval by the Principal.
- e. Present findings at scientific meetings, educational conferences, and other public forums as appropriate. All materials to be presented shall be approved by the Managing PI. All materials to be published shall be reviewed by one independent (separate from authors) reviewer and approved by the managing PI.
- f. The Utah FORGE website at <http://www.forgeutah.com/> will contain current information about seismicity at the site, including links to live seismographs like <http://www.quake.utah.edu/station/heli/FORU.png> and seismic event monitoring at <http://quake.utah.edu>.
- g. The Utah FORGE Facebook page, and other social media sites that may be developed, will disseminate information and receive feedback about project activity and seismic data.
- h. To ensure quality, press releases shall be submitted and reviewed by the Outreach Coordinator and Managing PI for approval by the Utah FORGE Project Management Team (PMT). PMT approval is required before the material is released.
- i. All printed and digital materials shall include, at a minimum the Utah FORGE logo and an acknowledgement of DOE funding.

Communication with DOE

The Managing PI will serve as the primary contact and will assume responsibility for ensuring open communication between the Utah FORGE team and the DOE.

- a. The Utah FORGE team will follow the communications guidelines provided by the GTO.
- b. Seismic monitoring and activity updates will be included in regularly occurring conference calls with the DOE and their technical monitoring team, as outlined in the Communications and Outreach Plan of this report.
- c. All seismic mitigation reports shall be submitted in accordance with the Federal Assistance Reporting Checklist and its corresponding instructions. All reports will be submitted by the managing PI in a timely fashion following the DOE format.
- d. The Managing PI shall provide the Geothermal Technologies Office (GTO) a courtesy copy of all press release materials for review. GTO comments and edits will be carefully considered prior to release.
- e. The outreach coordinator will inform the GTO of website and social media posts related to seismic monitoring and activity.

Student Educational Outreach Activities

The Utah FORGE team recognizes great value in teaching through engaging students and teachers in active, cutting-edge science and technology. We will conduct outreach activities

tailored to specific educational levels. Outreach activities will be made available to local and national students. In addition to the activities listed above, seismicity will be included in the educational outreach activities detailed in the Communications and Outreach Plan.

Emergency Contacts

Additional contacts are included under Task 1.3.2. Environmental, Safety and Health Plans.

Beaver County Sheriff
26 S 100 West
Milford, UT 84751
Milford Dispatch (435) 387-2758
Dispatch@BeaverUtahSheriff.com
Emergency 911

Beaver County Fire
District #2
26 S 100 West
Milford, UT 84751
(435) 387-2620
Fire Chief Cell (435) 691-2381
Emergency 911

Milford Valley Memorial Hospital
850 North Main Street,
UT Highway 257
Milford, Utah 84751
(435) 387-2411
Emergency 911

Wildland fires-
Richfield Interagency Fire Center
(435) 896-8404
Emergency 911

3. Criteria for Ground Vibration and Noise

This section of the report will be addressed in Phase 2B. Given the nearby quarry, railway and airport traffic, the ground vibration and noise from the more distant Utah FORGE site is expected to be negligible. However, in Phase 2 we will collect appropriate data to establish background rates in order to quantify existing ground vibration and noise sources for comparison to potential EGS development scenarios.

4. Local Seismic Monitoring

Collect unbiased (time and space) seismic data in the vicinity of the Utah FORGE project

Seismic activity in the area surrounding the Utah FORGE site has been actively monitored by a regional seismic network run by UUSS since 1981. Event locations and magnitudes are captured in the UUSS catalog (discussed below in more detail in Section 5). Analysis of this catalog for

the time period 1 January 2000 to 30 June 2003 found a minimum magnitude of completeness (M_{comp}) for the Utah FORGE site of M_{comp} 1.5 (Pankow et al., 2004). Since that analysis, regional seismic station coverage has improved in the region. Based on network coverage, the current M_{comp} is at least 1.5.

To push the M_{comp} to M 0 or lower magnitudes, in Phase 2A, we will install a five station local, surface seismic network. This array will operate for the duration of Phases 2A and 2B. Seismicity rates are very low in this area, so the deployment duration must be greater than the minimum one month DOE requirement in order to collect an adequate background data set. Data from this temporary network will be combined with data from the regional seismic network in order to locate and determine magnitudes for any new seismic events. At the same time that we install the surface telemetered seismic array, we will also install a stand-alone dense (40 to 90 station) Nodal seismic array across the top and adjacent to the Utah FORGE site for a minimum of one month. Data from the Nodal seismometers will not be telemetered. The Nodal data will be analyzed following the deployment using sophisticated array detection algorithms to look for additional small seismic events. The dense spacing of seismometers in the Nodal deployment will allow for precise locations in three-dimensions. Locations and detections found with the Nodal array will also be used to determine templates and station delays to improve detections and locations for seismic events recorded on the telemetered network. The geometry of the Nodal array will be designed to collect data for seismic tomography work and to measure the average shear velocity in the upper 30 m for at least one site. Data collection and seismic event detection and location will take place in Phase 2A. The tomography and shallow shear wave velocity analysis will be completed in Phase 2B.

Network array design to capture all aspects of seismicity

In Phase 2C, a permanent local seismic network will be installed. In the preliminary planning, we are proposing to: (1) add three or more additional surface stations on the perimeter of the basin; and (2) add 4-8 borehole seismometers in the basin. The borehole sensors are necessary to accurately locate small magnitude seismicity related to reservoir development. These borehole instruments will allow for a M_{comp} below zero. The location of the boreholes will depend on the final drilling plan. We anticipate one ring of 4 seismometers approximately 1 km from the bottom hole locations of the wells and a second ring located at a distance of 2 km. The surface array will allow for more regional monitoring of seismicity to identify if seismic activity is migrating outside of the borehole instrumentation footprint or if the seismicity is tracking outside of the proposed Utah FORGE area towards known fault structures.

In addition to the local network array that will run in real-time (telemetered continuous data), we also propose to use the Nodal seismic system to monitor reservoir development during some of the stimulation stages. This data will not be in real-time, but will be processed in a time frame that can be used to instruct the next stage of reservoir development. There will also be a network of downhole seismometers within the deep well site to improve fracture imaging as the reservoir is created.

Minimum data processing: location, magnitude and source mechanism

Data from the Utah FORGE project will be folded into routine seismic event processing at UUSS. Data will flow into an Advanced National Seismic System (ANSS) Quake Monitoring System (AQMS). From this system, events will be automatically located and magnitudes will be

determined (local magnitude, M_L , duration magnitude, M_C , and moment magnitude, M_w when possible), in near-real-time. The automatic solutions will be used to issue alarms based on criteria developed as part of this project. The automatic solutions will be reviewed by analysts to determine final location and magnitude. If larger events ($M > 3.5$) occur, waveform full moment tensors (Minson and Dreger, 2008; Whidden and Pankow, 2012) will be determined. For smaller events, first motion focal mechanisms can be determined. In Phase 2B, we will also look into other methods for source mechanism determination for small events that can be incorporated into routine processing.

In addition to the standard earthquake source products described above, we will also generate ShakeMaps for earthquakes $M > 2.5$. ShakeMaps are not usually made for such small events, but generating these maps will allow us to best monitor potential nuisance events. The maps can also be used for outreach to clearly describe the extent of shaking from any induced earthquake.

Maintain monitoring throughout injection activity

The seismic network described above will be maintained throughout the lifetime of the project. The data from the local array will be used in conjunction with the regional seismic network and at the end of the project the two datasets will be used to determine to what extent and with what instrumentation monitoring will continue past the end of the project.

In addition to the earthquake monitoring system, we will also install an accelerometer at Milford High School. This instrument will help inform about ground motions in the closest town and can be used in outreach efforts. The regional seismic network (UUSS) already has accelerometers located in Beaver, the next closest town to the proposed site. The accelerometer data is telemetered to the UUSS and is archived at IRIS.

5. Hazard from Natural and Induced Seismic Events (Before stimulation)

Estimate hazard from natural seismicity

Evaluate historical catalog

To evaluate the historical seismicity, we review three relevant earthquake catalogs: (1) a uniform moment magnitude catalog (1850- September, 2012; Arabasz et al., 2015); (2) the microseismic catalog (August, 1979 – summer 1981) collected by Zandt et al. (1982); and (3) the UUSS earthquake catalog, 1981-2015. For all three catalogs, seismicity near the Utah FORGE site is described as low-magnitude and low-frequency. Using the Arabasz et al. (2015) catalog, we see that the largest event in the study area (M_w 4.08) occurred in 1908 and was located south of Milford (Figures 1 and 3). The closest substantial earthquake ($M > 6$) occurred in 1901 in the Tushar Mountains north of Beaver ~75 km to the northeast of the Utah FORGE site.

Before production at Roosevelt Hot Springs began, Zandt et al. (1982) installed a local seismic array to detail the background seismicity. During the approximate 2 year deployment, they concluded there were few earthquakes $M > 2$. They did capture one energetic seismic swarm (1044 earthquakes $M \leq 1.5$) during June through August, 1981. This swarm occurred east of the present borefield at Roosevelt Hot Springs, primarily in the Mineral Mountains (Figure 3). The trend of the seismicity was mostly east-west. They concluded that the swarm was primarily naturally occurring and was consistent with either (or both) seismicity occurring along the

projection of the east-west trending Negro Mag fault or along northwest trending faults mapped by Nielson et al. (1978). A few of the earthquakes located on the west end of the swarm may have occurred along the Opal Mound Fault, but this interpretation remains speculative.

In support of the Utah FORGE project, events in the UUSS catalog (1981-2015) were relocated using updated velocity models, with depths set relative to sea level (Figure 3). The relocation of the events caused slight changes in location, but overall provided tighter clustering spatially. From the relocated events, it is observable that no events (within the current M_{comp} 1.5; Pankow et al., 2004) located within the proposed Utah FORGE deep drilling and office footprint (Figure 1). Earthquakes occurring outside this footprint during 1981-2015 range from M -0.09 to 3.91. The average horizontal and vertical 90% confidence errors for these earthquakes are 0.879 km and 4.863 km, respectively. Spatially there are two distinct clusters, to the north and northwest of Milford. In addition, there is a diffuse region of seismicity east of the Utah FORGE site in the Mineral Mountains (Figure 3).

Waveform analysis and event timing indicates that events in the northwest cluster (outlined by the blue ellipse in Figure 3) are the result of quarry blasts, not tectonic earthquakes. Evidence for this conclusion includes their epicentral proximity to quarries (conspicuous on Google maps), small magnitudes (M 0.49 to 2.05), shallow depths, restricted timing (all events occur during daylight hours), and highly correlated waveforms implying a similar location and source mechanism. The second cluster outlined by the green ellipse (Figure 3) is located near the Milford airport and not far from the M_w 4.08 1908 Milford earthquake, the largest recorded earthquake in the study area. The magnitudes in this cluster range from 0.46 to 3.91, and the events occur throughout the day (without a time bias). This cluster is interpreted as tectonic in origin.

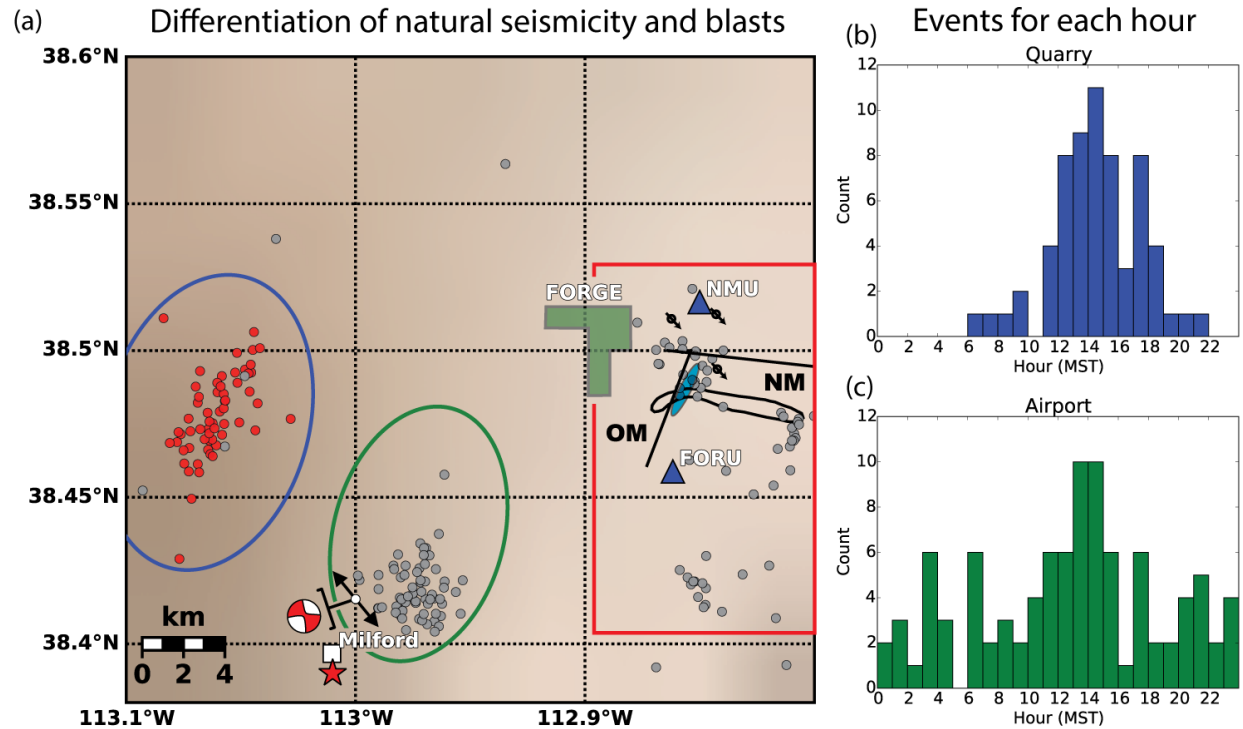


Figure 3. The relocated earthquake catalog. (a) Differentiation between natural seismic events and quarry blasts for UUSS catalog 1981 – 2015. Red and gray circles represent blasts and natural seismicity, respectively. The blue and green ellipse outlines refer to the events within the histograms. The red outline represents the Mineral Mountains study area. The black lines in the Mineral Mountains study area represent the Opal Mound (OM) and Negro Mag (NM) fault. The NM fault continues off the study area to the east. The black outline, overlapping the OM fault, represents the area of the Zandt swarm (Zandt et al. 1982). The blue triangles are seismic stations; the green polygon represents the Utah FORGE deep drill site. The black circles with an arrow through them, east of the FORGE drilling footprint, represent injection wells for the Blundell geothermal plant. The blue ellipse, east of the OM fault, represents the production well area for the Blundell geothermal plant. The white square represents the center of Milford, UT and the red star is the epicenter of the 1908 earthquake, M 4.08. The white circle represents the April 10, 1998 ML 3.91 earthquake with T-axis and focal mechanism (displayed offset from T-axis). (b) shows events within the blue ellipse as a function of time of day (these events occurring during daylight hours) and (c) shows seismicity located in the green ellipse (these events occur during all hours of the day). Based on the time of day and the proximity to quarries, 62 of the 201 events displayed are classified as blasts.

Of the remaining seismicity located in the Mineral Mountains (outlined by the red box in Figure 3), most locates east of the Opal Mound Fault. There is no evidence in the UUSS catalog for extensive swarm activity (Figure 4). Spatially there is some clustering of events around the Opal Mound Fault and clustering on the eastern edge of the Zandt 1981 swarm, and a third cluster further to the south (Figure 3). Waveform clustering analysis (Chambers et al., 2015) indicates that there are several distinct clusters of seismic events in the Mineral Mountain area (Figure 5).

Based on the different clusters and the proximity to the Roosevelt Hot Springs geothermal

system, we investigated possible correlations with the pumping history related to power production at the Blundell Power Plant. The plant was commissioned in 1984 and ramped up to full production and injection levels by 1986. Since then, the plant typically produces about 20 billion pounds of hot water at 250°C per year (9 million metric tons, or about 7500 acre-feet at 100°C), and it injects about 17 billion tons (7.7 million metric tons, or about 6500 acre-feet). The difference is mostly the mass of water evaporated in forced-draft cooling towers (Allis and Larsen, 2012). This deficit caused a pressure decline in the reservoir of about 4 MPa (about 600 psi) mostly in the first few years of (refer to Task 1.3.3 Update of Seismicity Data, for more detailed information). No observable connection to the events cataloged in the area and the injection/withdrawal history of the power plant was observed (Figure 6). There is only one event cataloged from completion of the plant to 1992. A binary power plant was brought on line in 2007 (allowing more heat to be extracted from the recovered fluids) but there was no visible change in the seismic activity. No events were located from April 2011 through January 2016 in the Mineral Mountains study area.

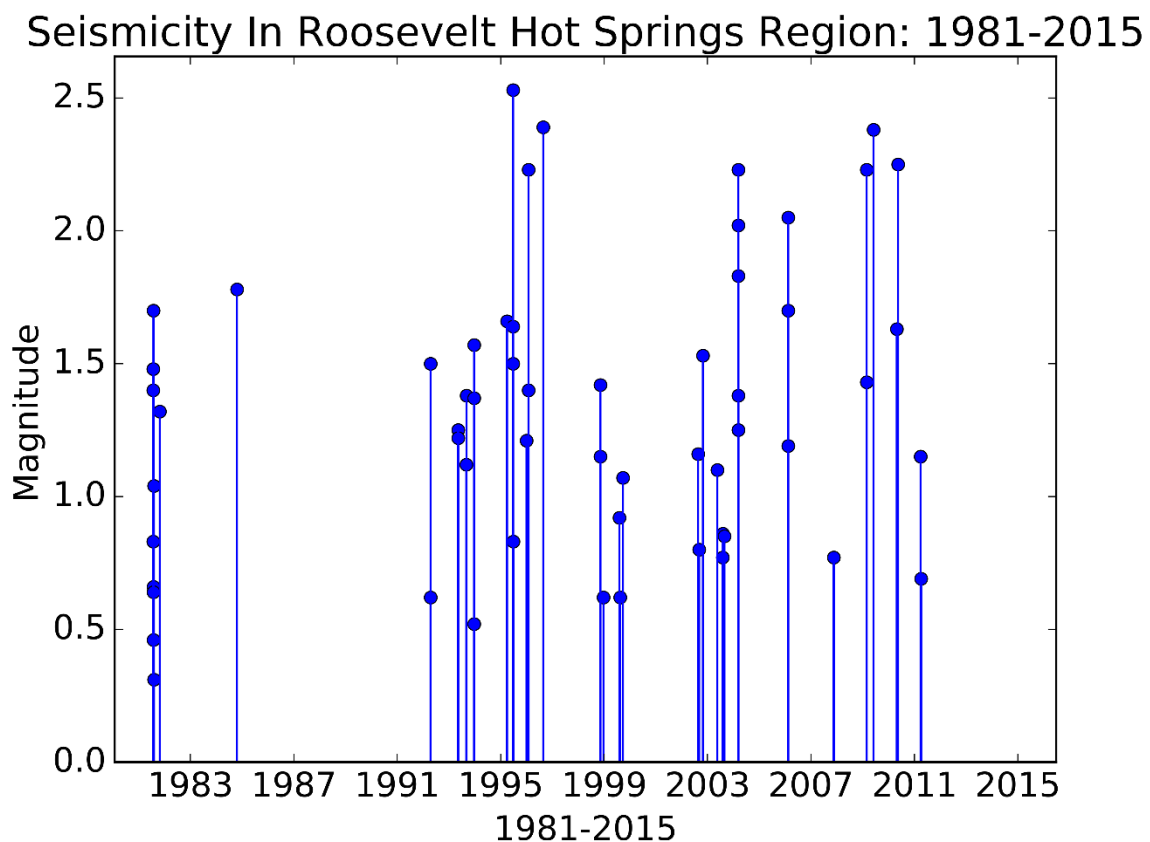


Figure 4. *Magnitude vs. time plot for events in the red outline in Figure 3. Notice the seismically quiet time periods from October of 1984 through April 1992 and April 2011 through 2015. The group of seismicity in 1981 is part of the swarm described by Zandt et al. (1982). The data held by the Division of Water Rights is incomplete and in places incorrect, so a correction has been applied based on the gross MW-h produced each year and an assumption of constant production.*

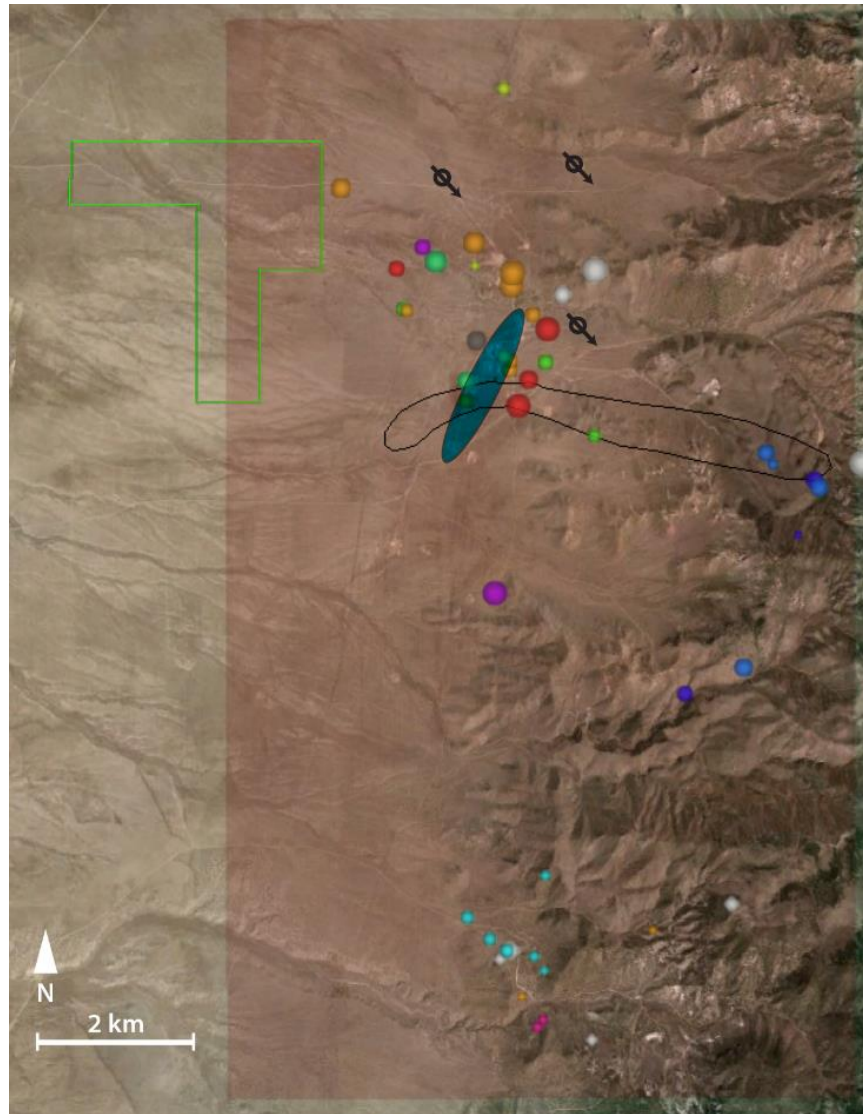


Figure 5. Screenshot of Google Earth Pro with colors representing clustered waveforms, from original catalog data, based off of similarity from the Detex program suite. There are many various clusters of similar waveform, as seen by the different colors. The Utah FORGE area is outlined in green. The black circles with an arrow through them, east of the FORGE drilling footprint, represent injection wells for the Blundell geothermal plant at the Roosevelt Hot Springs geothermal system. The blue ellipse represents the production well area for the Blundell geothermal plant. The injection and production well symbols are not a part of the KML product and were added to the figure for clarity.

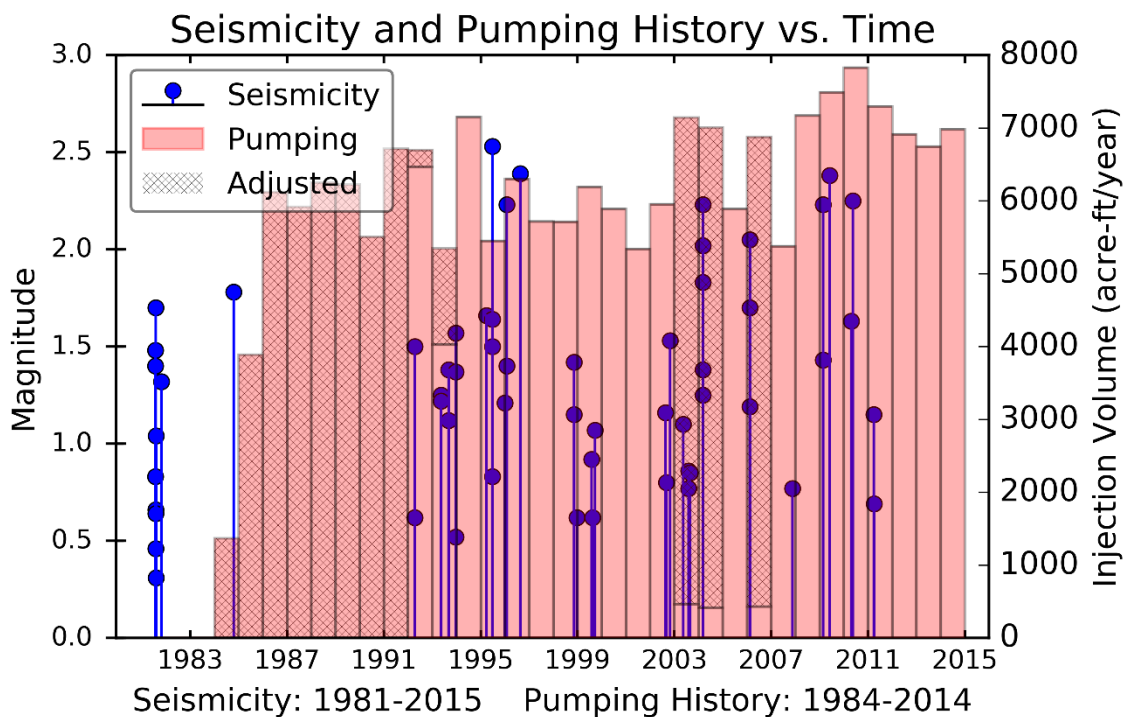


Figure 6. Magnitude vs. time plot of events in the red outline in Figure 1, with Blundell power plant injection history compiled from Utah Division of Water Rights website. The injection data was incomplete and in places incorrect, so a correction has been applied based on the gross MW-hours produced each year and an assumption of constant production enthalpy (“adjusted” numbers). Note the seismically quiet time periods from October 1984 through April 1992 and April 2011 through 2015. The seismicity occurring in 1981 is part of the swarm described by Zandt et al. (1982). See text for volume conversions. For simplicity, 6500 acre-ft is 2.1 million gallons.

Characterize any active or potentially active fault and estimate source parameters

The area adjacent to the Utah FORGE site, including the Mineral Mountains has been mapped in detail by Nielson et al. (1978). In the immediate area surrounding the Utah FORGE site, there are two mapped faults; the Opal Mound fault and the Negro Mag fault (Figure 3). The Opal Mound fault separates the convective thermal regime of the Roosevelt Hot Springs geothermal system from the conductive thermal regime of the Utah FORGE site. Both the Opal Mound and Negro Mag faults have clear surface expressions. The distribution of subsurface structures is, at this point, poorly understood. A detailed reflection seismic survey, and other geophysical surveys will be conducted in Phase 2 to locate buried and poorly exposed structures that could impact the Utah FORGE project.

The lengths of the mapped traces of the Opal Mound fault and the Negro Mag fault (Figure 3) are 4.72 km and 10.6 km, respectively. Assuming this entire length ruptures in a normal faulting event, the maximum magnitude for these faults are calculated to be M 5.4 and M 5.9 (Wells and Coppersmith, 1994). These moderate sized magnitudes are consistent with the lack of well-defined scarps.

Geologic site conditions and shallow shear-wave velocity

Currently for use in ShakeMap, UUSS uses a generalized shear-wave velocity map based mainly on mapped geologic units (<http://quake.utah.edu/monitoring-research/uuss-urban-strong-motion-network/geological-site-conditions>). The average shear-wave velocity in the upper 30 m (V_{s30} values) for each unit are based on V_{s30} measurements collected for the Wasatch Front in northern Utah (McDonald and Ashland, 2008). There are no site-specific shallow shear-wave velocity data for the region around the Utah FORGE site or for the nearby town of Milford. This data will be collected in Phase 2 of this project.

Select appropriate ground-motion prediction models

For earthquakes with magnitudes greater than M 5, UUSS currently uses the Chiou and Youngs (2008) ground motion prediction equation to generate deterministic scenarios. Unfortunately, data from normal faulting earthquakes is scarce for Basin and Range earthquakes. This lack of data makes objectively evaluating different ground motion equations difficult. In Phase 2, we will investigate the new NGA 2014 ground motion prediction relations (e.g. Gregor et al., 2014).

Perform a PSHA and produce hazard curves

To begin the PSHA analysis, we start with the 2008 U.S. Geological Survey (USGS) National Seismic Hazard Map (NSHM; Peterson et. al., 2008) and tools provided on the USGS website (Figure 2) to get a regional perspective of the hazard. From this analysis the hazard from natural seismicity is low to moderate.

As part of Phase 2, we will look at changes in the 2014 NSHM to see how the probabilistic regional hazard has changed. We will also perform a site-specific PSHA analysis for magnitudes down to M 4, as suggested by Majer et al. (2012).

Estimate hazard from induced seismicity

Develop 3D model of geothermal area

For a detailed review of the 3D model developed for the Utah FORGE site see Task 1.2.

Review known cases of induced seismicity and compare tectonic framework

Induced seismicity has been associated with many human activities: dam impoundment (e.g. Simpson et al., 1988), mining activities (e.g. Gibowitz et al. 2009), deep injection of waste fluids (e.g. Healy et al., 1968), and injection related to geothermal production (e.g. Majer et al., 2007). While the mechanisms in all these cases might be similar, perhaps related to volume change (McGarr, 1976), there are differences. For example, it has been observed that maximum magnitudes related to geothermal stimulation are larger than magnitudes from fracking associated with hydrocarbon recovery (Shapiro et al. 2011). An exception to this is the 2015 M 4.6 induced earthquake in Alberta, Canada (Wang et al., 2016).

A thorough review of all known induced seismicity sources is beyond the scope of this project. However, a review of induced seismicity associated with enhanced geothermal stimulation (EGS) is presented here. An Enhanced Geothermal System (EGS) is a manmade underground

heat exchanger designed to extract geothermal energy by circulating water between an injection well and production well through a series of fractures in the subsurface. Most often EGS systems have been developed in areas where there is hot low permeability rock near the Earth's surface, either on the periphery of natural geothermal systems or in areas where a preexisting geothermal resource did not exist. Techniques that have been investigated to increase the permeability of these rocks include: the use of explosive charges; high-pressure and high injection rate hydraulic stimulations; long-term injection/circulation of cool fluids; and chemical stimulations that typically involve the use of acid. The first EGS project was conducted at Fenton Hill, New Mexico in 1974. Subsequently EGS projects have been conducted in North and Central America, Europe, Japan and Australia.

Induced seismicity has been documented in operating geothermal fields and EGS projects. In the most significant of these, thousands of small events are generated annually. These are predominantly microearthquakes (MEQs) not felt by people, but also include earthquakes of magnitudes up to the 4–5 range. At other sites, the induced seismicity may be entirely of very low magnitudes, or a short-lived transient phenomenon. These MEQ events have led to little or no damage in most of the operating hydrothermal fields around the world (Majer et al., 2007).

Induced seismicity in geothermal environments is the result of: pore-pressure increases that result in effective stress reduction; temperature decreases that result in the contraction of fracture surfaces; volume changes due to fluid withdrawal/injection resulting in a perturbation of the local stress field; and chemical alteration of fracture surfaces that change the coefficient of friction (Majer et al., 2007). The extent and degree to which these subsurface phenomena are active is the result of: orientation and magnitude of the deviatoric stress field in relation to existing faults; the extent of faults and fractures; and the area of fault slippage and stress drop across a fault (Majer et al., 2007).

A literature search was conducted to determine factors that influenced micro-seismicity in previous EGS projects. Factors that may be of relevance include: depth of stimulation, formation temperature and rock type; stimulation types (hydraulic, long-term circulation and chemical); and stimulation parameters such as injected fluid volume, well head pressure, injection rate and duration of injection/circulation. Summaries of EGS systems and their enhanced seismicity have been presented by Tester et al. (2006), Majer et al. (2007), Ghassemi et al. (2010), Bromely and Majer (2012) and Breede et al. (2013). More recent developments in later/ongoing EGS projects have been pulled from the literature (Table 1).

The majority of EGS projects have targeted crystalline basement rocks (intrusive and metamorphic) with less common stimulations of volcanic and sedimentary rock. Types of stimulations have been categorized as hydraulic, long-term circulation, chemical and explosive. Hydraulic stimulations create fractures using high injection pressures and high injection rates for a relatively short period of time. Long-term stimulations create fractures using lower injection pressures and injection rates over longer periods of time, and usually involve the injection of cool water into hot rock. Chemical stimulations involve the use of acid to dissolve rock to create permeability. Explosive stimulations have been conducted at one site, Rosemanowes, U.K. The use of a combination of stimulation types is common. The depth of stimulated wells range from 450 to 5084 m (Figure 7), and formation temperatures at EGS sites have ranged from as low as 33°C to as high as 400°C (Figure 8). Stimulation parameters such as well-head pressure (WHP),

maximum flow rate, volume of injected fluids and duration of injection are summarized in Figure 9. Seismicity associated with EGS projects in summarized in Figure 10

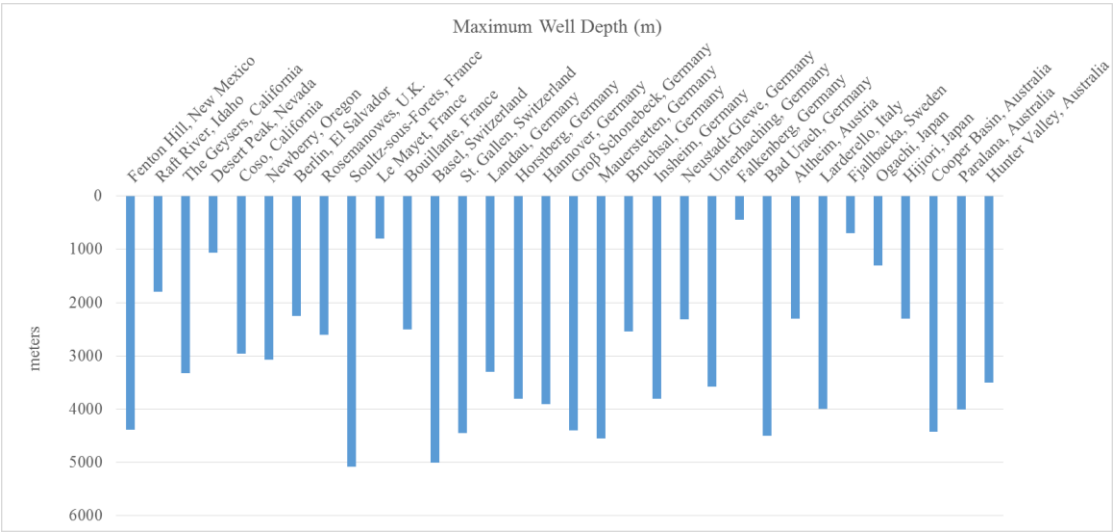


Figure 7: Maximum depth of EGS wells by site as reported in the literature.

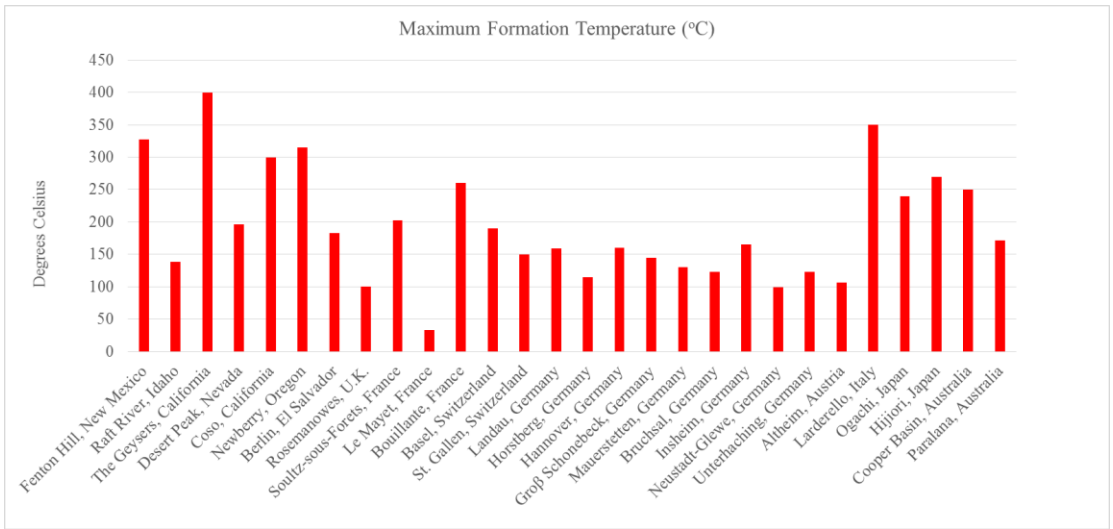


Figure 8: Maximum formation temperatures at EGS sites as reported in the literature.



Figure 9: Maximum well head pressure (WHP), maximum flow rates, injected volume and injection duration by EGS site as reported in the literature.

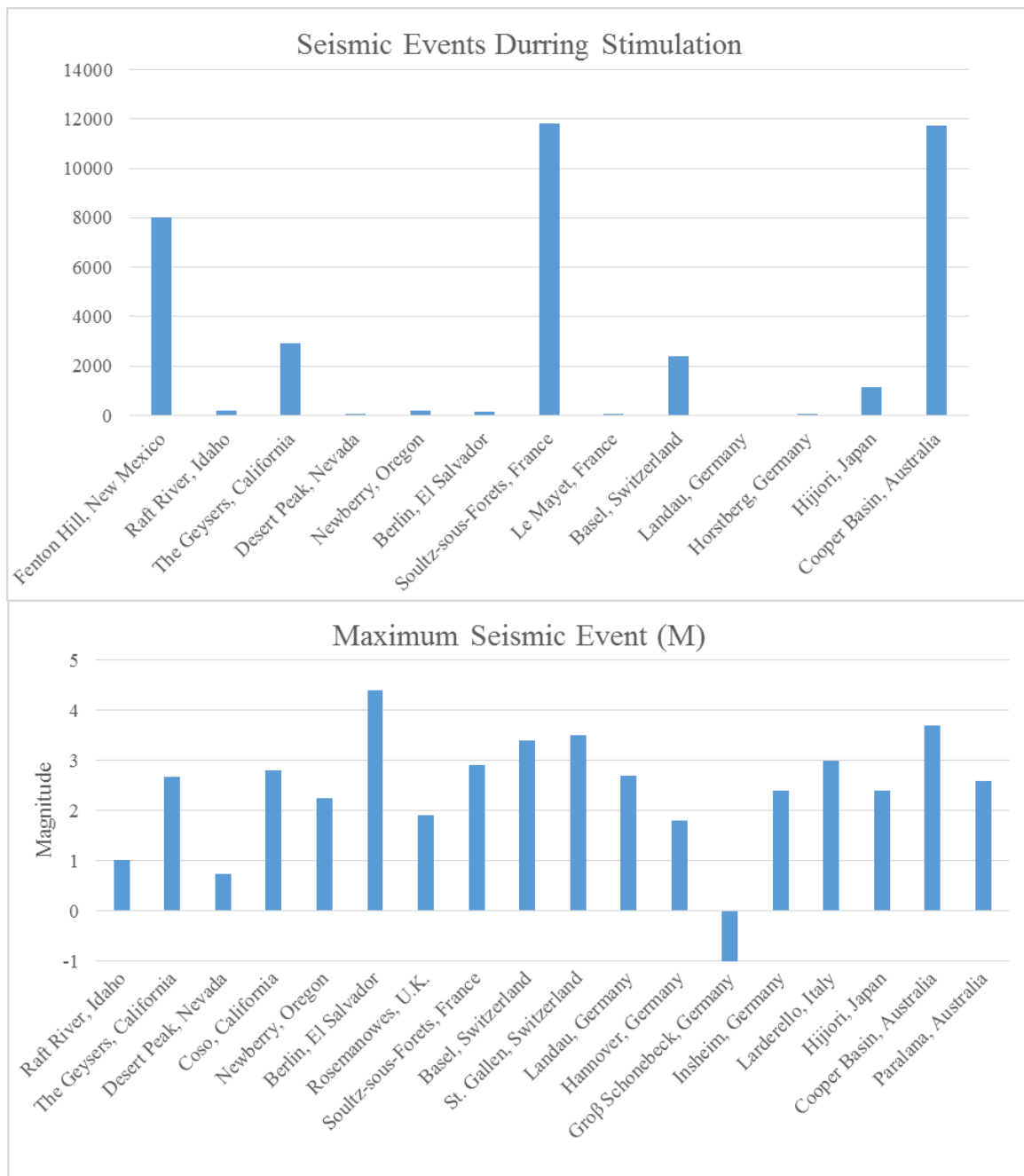


Figure 10: Published seismicity data for EGS projects.

	Regional Stress Regime NF = normal faulting SS = strike slip faulting TF = thrust faulting	Target Formation: intrusive (Int) metamorphic (Mm) sedimentary (Sed) volcanic (Vol)	Maximum well depth (m)	Maximum measured formation temperature (°C)	Stimulation Type: hydraulic (Hyd) long-term injection (L-T) chemical (Chem)	Number of seismic events during stimulation	Max seismic event during stimulation (magnitude)	Well head pressure (WHP) MPa	Volume of injected fluid (m³)	Maximum injection rate (l/s)	Injection duration (years)
Fenton Hill, New Mexico	NF (Brown, 2009)	Int & Mm (Brown, 2009)	4390 (Tester et al., 2006)	327 (Ghassemi et al., 2010)	Hyd & L-T (Ghassemi et al., 2010)	8,000 (Bromley and Majer, 2012)		30.3 (Tester et al., 2006)	> 37,000 (Tester et al., 2006)	18.5 (Tester et al., 2006)	1.681 (Ghassemi et al., 2010)
Raft River, Idaho	NF (Williams et al., 1982)	Mm (Jones et al., 2011)	1800 (Jones et al., 2011)	138 (Jones et al., 2011)	Hdy & L-T (Bradford et al., 2016)	185 (Bradford et al., 2016)	1.01 (Bradford et al., 2016)	7.9 (Bradford et al., 2016)	2,000,000 (Bradford et al., 2016)	63.1 (Bradford et al., 2016)	3.833 (Bradford et al., 2016)
The Geysers, California	NF (Oppenheimer, 1986)	Mm (Garcia et al., 2012)	3326 (Rutqvist et al., 2015)	400 (Garcia et al., 2012)	L-T (Garcia et al., 2012)	2,919 (Garcia et al., 2012)	2.67 (Garcia et al., 2012)		1,135,500 (Rutqvist et al., 2015)	75.7 (Rutqvist et al., 2015)	1.000 (Rutqvist et al., 2015)
Desert Peak, Nevada	NF (Chabora et al., 2012)	Vol (Chabora et al., 2012)	1067 (Chabora et al., 2012)	196 (Chabora et al., 2012)	Hdy, L-T & Chem (Chabora et al., 2012)	42 (Benato et al., 2013)	0.74 (Benato et al., 2013)	7.0 (Chabora et al., 2012)	344 (Chabora et al., 2012)	45.7 (Chabora et al., 2012)	0.115 (Chabora et al., 2012)
Coso, California	NF & SS (Walter and Weaver, 1980)	Int	2956 (Julian et al., 2009)	300 (Benato et al., 2013)	Hyd (Benato et al., 2013)		2.80 (Benato et al., 2013)	6.9 (Benato et al., 2013)		176.8 (Benato et al., 2013)	0.038 (Benato et al., 2013)
Newberry, Oregon	NF (Cladouhos et al., 2015)	Int & Vol (Osborn et al., 2011)	3066 (Osborn et al., 2011)	315 (Cladouhos et al., 2015)	Hyd (Cladouhos et al., 2015)	175 (Cladouhos et al., 2015)	2.26 (Cladouhos et al., 2015)	19.7 (Osborn et al., 2011)	54,500 (Cladouhos et al., 2015)	3.8 (Cladouhos et al., 2015)	0.200 (Osborn et al., 2011)
Berlin, El Salvador	SS & NF (Kwaitek et al., 2014)	Vol (Horio-Henriquez, 2007)	2248 (Kwaitek et al., 2014)	183 (Kwaitek et al., 2014)	Hyd (Kwaitek et al., 2014)	134 (Kwaitek et al., 2014)	4.40 (Bommer et al., 2006)	13.3 (Kwaitek et al., 2014)		159.0 (Kwaitek et al., 2014)	0.156 (Kwaitek et al., 2014)
Bouillante, Guadeloupe	NF (Traineau et al., 1997)	Vol (Correia et al., 2000)	2500 (Correia et al., 2000)	250 (Correia et al., 2000)	L-T (Correia et al., 2000)	0 (Correia et al., 2000)		2.5 (Correia et al., 2000)		25 (Correia et al., 2000)	0.047 (Correia et al., 2000)

Rosemanowes, U.K.	SS (Kolditz and Clauser, 1998)	Int (Bromley and Majer, 2007)	2600 (Ghassemi et al., 2010)	100 (Ghassemi et al., 2010)	Explosive, Hyd & L-T (Bromley and Majer, 2007; Ghassemi et al., 2010)		1.90 (Bromley and Majer, 2007)	14 (Ghassemi et al., 2010)		100.0 (Ghassemi et al., 2010)	4.000 (Ghassemi et al., 2010)
Table 1: Continued											
	Regional Stress Regime NF = normal faulting SS = strike slip faulting TF = thrust faulting	Target Formation: intrusive (Int) metamorphic (Mm) sedimentary (Sed) volcanic (Vol)	Maximum well depth (m)	Maximum measured formation temperature (°C)	Stimulation Type: hydraulic (Hyd) long-term injection (L-T) chemical (Chem)	Number of seismic events during stimulation	Max seismic event during stimulation (magnitude)	Well head pressure (WHP) MPa	Volume of injected fluid (m³)	Maximum injection rate (l/s)	Injection duration (years)
Soultz, France	SS & NF (Dobarth et al., 2009; Evans et al., 2012)	Int (Evans et al., 2005)	5084 (Concha et al., 2010)	202 (Majer et al., 2007)	Hdy, L-T & Chem (Concha et al., 2010; MIT; Majer et al., 2007; Dobath et al., 2009)	11,809 (Concha et al., 2010)	2.9 (Concha et al., 2010)	17.0 (Dorbath et al., 2009)	162,280 (Dobath et al., 2009; Evans et al., 2005)	100.0 (Dorbath et al., 2009)	0.459 (Dobath et al., 2009; Evans et al., 2005)
Le Mayet, France	NF (Evans et al., 2012)	Int (Tester et al., 2006)	800 (Tester et al., 2006)	33 (Breede et al., 2013)	Hyd & L-T (Tester et al., 2006)	35 (Breede et al., 2013)	“Not felt” (Evans et al., 2012)	25 (Evans et al., 2012)	200 (Evans et al., 2012)	73.0 (Breede et al., 2013)	
Basel, Switzerland	SS (Haring et al., 2008)	Int (Haring et al., 2008)	5000 (Haring et al., 2008)	190 (Haring et al., 2008)	Hyd & L-T (Haring et al., 2008)	2,400 (Haring et al., 2008)	3.40 (Haring et al., 2008)	29.6 (Haring et al., 2008)	11,570 (Haring et al., 2008)	55.0 (Haring et al., 2008)	0.016 (Haring et al., 2008)
St. Gallen, Switzerland	SS (Moeck et al., 2015)	Sed (Moeck et al., 2015)	4450 (Moeck et al., 2015)	150 (Moeck et al., 2015)	Hyd, L-T & Chem (Kiraly et al., 2014)	340 (Kiraly et al., 2014)	3.50 (Moeck et al., 2015)		> 700 (Kiraly et al., 2014)		.077 (Moeck et al., 2015)
Landau, Germany	NF (Schinkler et al., 2010)	Int & Sed (Schinkler et al., 2010)	3300 (Schinkler et al., 2010)	159 (Breede et al., 2013)	Hyd, L-T & Chem (Schinkler et al., 2010)	0 (Schinkler et al., 2010)	2.70 (Schinkler et al., 2010)	13.0 (Schinkler et al., 2010)	11,300 (Schinkler et al., 2010)	190.0 (Schinkler et al., 2010)	2.000 (Schinkler et al., 2010)
Horstberg, Germany	SS (Evans et al., 2012)	Sed (Tester et al., 2006)	3800 (Tester et al., 2006)	115 (Tester et al., 2006)	Hyd (Tester et al., 2006)	5 (Tester et al., 2006)	<0 (Evans et al., 2012)	33.0 (Tester et al., 2006)	20,000 (Tester et al., 2006)	50.0 (Tester et al., 2006)	

Hannover, Germany	TF (Heidbach et al., 2008)	Sed (Breede et al., 2013)	3900 (Breede et al., 2013)	160 (Breede et al., 2013)	Hyd (Breede et al., 2013)		1.80 (Breede et al., 2013)				
Groß Schonebeck, Germany	NF (Kwiatek et al., 2010)	Sed & Vol (Breede et al., 2013)	4400 (Breede et al., 2013)	145 (Breede et al., 2013)	Hyd & Chem (Breede et al., 2013)	80 (Kwiatek et al., 2010)	-1.00 (Kwiatek et al., 2010)	59 (Evans et al., 2012)	13,000 (Evans et al., 2012)	150 (Evans et al., 2012)	
Mauerstetten, Germany	SS (Heidbach et al., 2008)	Sed (Breede et al., 2013)	4545 (Breede et al., 2013)	130 (Breede et al., 2013)	Hyd & Chem (Breede et al., 2013)						
Table 1: Continued											
	Regional Stress Regime NF = normal faulting SS = strike slip faulting TF = thrust faulting	Target Formation: intrusive (Int) metamorphic (Mm) sedimentary (Sed) volcanic (Vol)	Maximum well depth (m)	Maximum measured formation temperature (°C)	Stimulation Type: hydraulic (Hyd) long-term injection (L-T) chemical (Chem)	Number of seismic events during stimulation	Max seismic event during stimulation (magnitude)	Well head pressure (WHP) MPa	Volume of injected fluid (m³)	Maximum injection rate (l/s)	Injection duration (years)
Bruchsal, Germany	NF & SS (Meixner et al., 2014)	Sed (Breede et al., 2013)	2542 (Meixner et al., 2014)	123 (Breede et al., 2013)			none reported (Evans et al., 2012)	0.5 (Evans et al., 2012)		24 (Evans et al., 2012)	
Insheim, Germany	NF (Heidbach et al., 2008)	Int & Sed (Breede et al., 2013)	3800 (Breede et al., 2013)	165 (Breede et al., 2013)			2.40 (Breede et al., 2013)				
Neustadt-Glewe, Germany	SS (Evans et al., 2012)	Sed (Breede et al., 2013)	2320 (Breede et al., 2013)	99 (Breede et al., 2013)	L-T (Evans et al., 2012)		0 (Evans et al., 2012)	0.8 (Evans et al., 2012)		31 (Evans et al., 2012)	
Unterhaching, Germany	SS & TF Evans et al., 2012)	Sed (Breede et al., 2013)	3580 (Breede et al., 2013)	123 (Breede et al., 2013)	Chem (Breede et al., 2013)		2.4 (Evans et al., 2012)	2.5 (Evans et al., 2012)		120 (Evans et al., 2012)	
Falkenberg, Germany	TF (Jung, 1989)	Int (Jung, 1989)	450 (Tester et al., 2006)		Hyd & L-T (Tester et al., 2006)	16 (Tester et al., 2006)		18 (Tester et al., 2006)	91 (Tester et al., 2006)	3.5 (Tester et al., 2006)	0.002 (Tester et al., 2006)
Bad Urach, Germany	SS & NF (Evans et al., 2012)	Mm (Evans et al., 2012)	4300 (Evans et al., 2012)	170 (Tenzer et al., 2004)	Hyd (Evans et al., 2012)		1.8 (Evans et al., 2012)	34 (Evans et al., 2012)	5,600 (Evans et al., 2012)	50 (Evans et al., 2012)	0.002 (Tester et al., 2006)

Altheim, Austria	SS & TF (Evans et al., 2012)	Sed (Breede et al., 2013)	2306 (Breede et al., 2013)	106 (Breede et al., 2013)	Hyd & Chem (Breede et al., 2013)			1.7 (Evans et al., 2012)		81 (Evans et al., 2012)	
Larderello, Italy	SS & NF (Evans et al., 2012)	Sed (Evans et al., 2012)	4000 (Breede et al., 2013)	350 (Breede et al., 2013)	Hyd & L-T (Breede et al., 2013)		3.00 (Breede et al., 2013)				
Fjallbacka, Sweden	TF (Evans et al., 2012)	Int (Tester et al., 2006)	700 (Tester et al., 2006)		Hyd (Tester et al., 2006)		-0.2 (Evans et al., 2012)	13 (Evans et al., 2012)	200 (Evans et al., 2012)	21 (Evans et al., 2012)	0.111 (Tester et al., 2006)
Table 1: Continued											
	Regional Stress Regime NF = normal faulting SS = strike slip faulting TF = thrust faulting	Target Formation: intrusive (Int) metamorphic (Mm) sedimentary (Sed) volcanic (Vol)	Maximum well depth (m)	Maximum measured formation temperature (°C)	Stimulation Type: hydraulic (Hyd) long-term injection (L-T) chemical (Chem)	Number of seismic events during stimulation	Max seismic event during stimulation (magnitude)	Well head pressure (WHP) MPa	Volume of injected fluid (m³)	Maximum injection rate (l/s)	Injection duration (years)
Ogachi, Japan	TF (Kaieda et al., 2005)	Int & Vol (Kaieda et al., 2005)	1300 Kaieda et al., 2005; Ghassemi et al., 2010	240 (Ghassemi et al., 2010)	Hyd & L-T (Ghassemi et al., 2010)			22 (Kaieda et al., 2005)	189,000 (Kaieda et al., 2005)	37.5 (Kaieda et al., 2005)	0.574 (Kaieda et al., 2005)
Hijiori, Japan	TF (Sasaki and Kaieda, 2000)	Int (Bromley and Majer, 2007)	2300 (Kaieda, H., 2014)	270 (Kaieda, H., 2014)	Hyd & L-T (Kaieda, H., 2014)	1,133 (Kaieda 2014; Bromley and Majer, 2012)	2.40 (Kaieda, H., 2014)	25.5 (Kaieda, H., 2014)	51,000 (Kaieda, H., 2014)	33.3 (Kaieda, H., 2014)	1.669 (Kaieda, H., 2014)
Cooper Basin, Australia	TF (Wyborn et al., 20005)	Int (Asanuma et al., 2005; Baisch et al., 2006)	4421 (Asanuma et al., 2005; Baisch et al., 2006)	250 (Tester et al., 2006)	Hyd & L-T (Asanuma et al., 2005; Baisch et al., 2006)	11,724 (Asanuma et al., 2005)	3.70 (Asanuma et al., 2005)	70 (Asanuma et al., 2005)	40,000 (Asanuma et al., 2005; Baisch et al., 2006)	48.0 (Asanuma et al., 2005; Baisch et al., 2006)	0.027 (Asanuma et al., 2005; Baisch et al., 2006)
Paralana, Australia	TF (Albaric et al., 2014)	Int & Mm (Albaric et al., 2014)	3963 (Albaric	171 (Breede et al., 2013)	Hyd (Breede et al., 2013)	7085 (Albaric et al., 2014)	3.5 (Albaric et al., 2014)	62 (Albaric	3000 (Albaric et al., 2014)	27 (Albaric et al., 2014)	0.014 (Albaric

			et al., 2014)					et al., 2014)			et al., 2014)
Hunter Valley, Australia	TF (Heidbach et al., 2008)		3500 (Tester et al., 2006)								

While not an EGS project, the Roosevelt Hot Springs geothermal system provides a potential analog for investigating induced seismicity at the Utah FORGE site. The Roosevelt Hot Springs system is located several kilometers to the east of the Utah FORGE site in the same reservoir rocks. Production and injection has been ongoing since 1984. Over 4.16×10^{10} total gallons of water have been injected with 70% into well 14-2, located adjacent to the Negro Mag fault near its intersection with the Opal Mound fault. Associated seismic activity is minimal (at least for $M_{comp} > 1.5$). The Opal Mound fault occurs between the Utah FORGE site and the Roosevelt Hot Spring system. Given the lack of any significant seismicity on this structure over the last 30 years of injection, it seems unlikely earthquakes will occur in response to injection at the Utah FORGE site on this structure.

Lessons related to potential induced seismic events learned from past EGS projects and from the Roosevelt Hot Springs geothermal system include:

- The maximum induced earthquake can be bounded by the volume of injected fluid (McGarr, 2014) and/or to the size and shape of the fluid-stimulated volume (Shapiro et al., 2011)
- Because the relation of volume of fluid injected and the affected rock volume changes with time, so does the maximum magnitude earthquake.
- The largest earthquake often occurs after shut-in (perhaps several years later) and away from the injection well (by potentially several > 10 kilometers) and often near the edge of the seismic cloud (Baisch et al., 2010)
- Rock failure associated with fluid injection can be tensile failure (Hubbert and Willis, 1957) or shear failure of pre-existing joint sets (Hubbert and Rubey, 1959) or both
- As seismicity tends to migrate away from the injection well, source types as well as b-values also change as the seismicity migrates to larger distances from the well (e.g. Zang et al., 2014 and references therein)

Evaluate geologic framework, characteristics and distribution of pre-existing faults

Characterize maximum dimensions of pre-existing faults

The two mapped faults in the study area include the Opal Mound fault and the Negro Mag fault. The lengths of the mapped traces of the Opal Mound fault and the Negro Mag fault (Figure 3) are 4.72 km and 10.6 km, respectively. Assuming this entire length ruptures in a normal faulting event, the maximum magnitude for these faults are calculated to be M 5.4 and M 5.9 (Wells and Coppersmith, 1994). These moderate sized magnitudes are consistent with the lack of well-defined scarps.

Review and evaluate models for induced seismicity that estimate the maximum magnitude

In an early work, McGarr (1976) used the volume of fluid injected or extracted (e.g. during mining) to determine maximum magnitude of induced earthquakes. He has recently updated this work for fluid injection induced earthquakes (McGarr, 2014). The new relation limits the maximum seismic moment to the product of the injected volume and the modulus of rigidity. In comparing this relation to many examples where volume and magnitude is known, the relation does an impressive job of bounding the maximum observed magnitude. In other studies, Shapiro et al. (2011) showed that the magnitude of induced earthquakes are comparable to the

interactions between preexisting faults and the crustal volume influenced by the pore pressure increase. Gishig (2015) showed that the maximum magnitude depends on fault properties, the orientation of the natural faults, and the stress field.

To estimate an upper bound on the maximum induced earthquake for the Utah FORGE site, we use the relation developed by McGarr (2014). In the stimulation phase for the Utah FORGE site, we anticipate a fluid injection volume of 3500 to 20,000 m³. The modulus of rigidity has been determined to be 2.85×10^{10} Pa (see Section 1.1) based on triaxial testing of core samples of the reservoir rocks. Using these values and the McGarr relation, we get a maximum moment of 5.7×10^{14} N m. This is equivalent to an M_w 3.8 earthquake. This magnitude is similar to the other EGS sites analyzed in the McGarr (2014) study.

Review and select empirical relations appropriate for small magnitude events

Pankow (2012) compiled ground motion data for all M 3 to 5 earthquakes recorded by the seismic network in Utah. Using PGA and PGV, she compared the data to ground motion prediction equations developed for $M < 5$ earthquakes by Chiou et al. (2010), Atkinson and Boore (2011), and TriNet (Wald et al., 2005). The Chiou et al. (2010) Southern California relations best fit the Utah data. There was a large distance bias in the Atkinson and Boore (2011) relation for both PGA and PGV and a distance bias for PGV for the TriNet relation.

Calculate scenario ground motions from the maximum induced seismic event

Deterministic scenarios have been generated using ShakeMap (Wald et al., 1999; Worden and Wald, 2016) for four possible seismic events: (1) a repeat of the 1908 M 4.08 Milford earthquake; maximum magnitude earthquakes based on fault length (Wells and Coppersmith, 1994); (2) an M 5.4 Opal Mound fault; (3) an M 5.9 Negro Mag fault earthquake; and (4) an M 4 induced earthquake (conservative estimate based on the maximum magnitude calculation) located at the Utah FORGE site (Figure 11). Scenarios for the $M > 5.0$ events were generated using Chiou and Youngs (2008) ground motion prediction equation (GMPE); for the M 4.0 induced events, the Chiou et al. (2010) Southern California GMPE was used. Site amplification factors based on a statewide Vs30 (average shear velocity in the upper 30 m) database (McDonald and Ashland, 2008) were used for all scenarios. The Vs30 clearly dominates the pattern of ground motions, as seen by the significantly larger amplitudes in the basin. The default Vs30 values used in this analysis are based on Vs30 measurements from northern Utah, which is dominated by lake sediment.

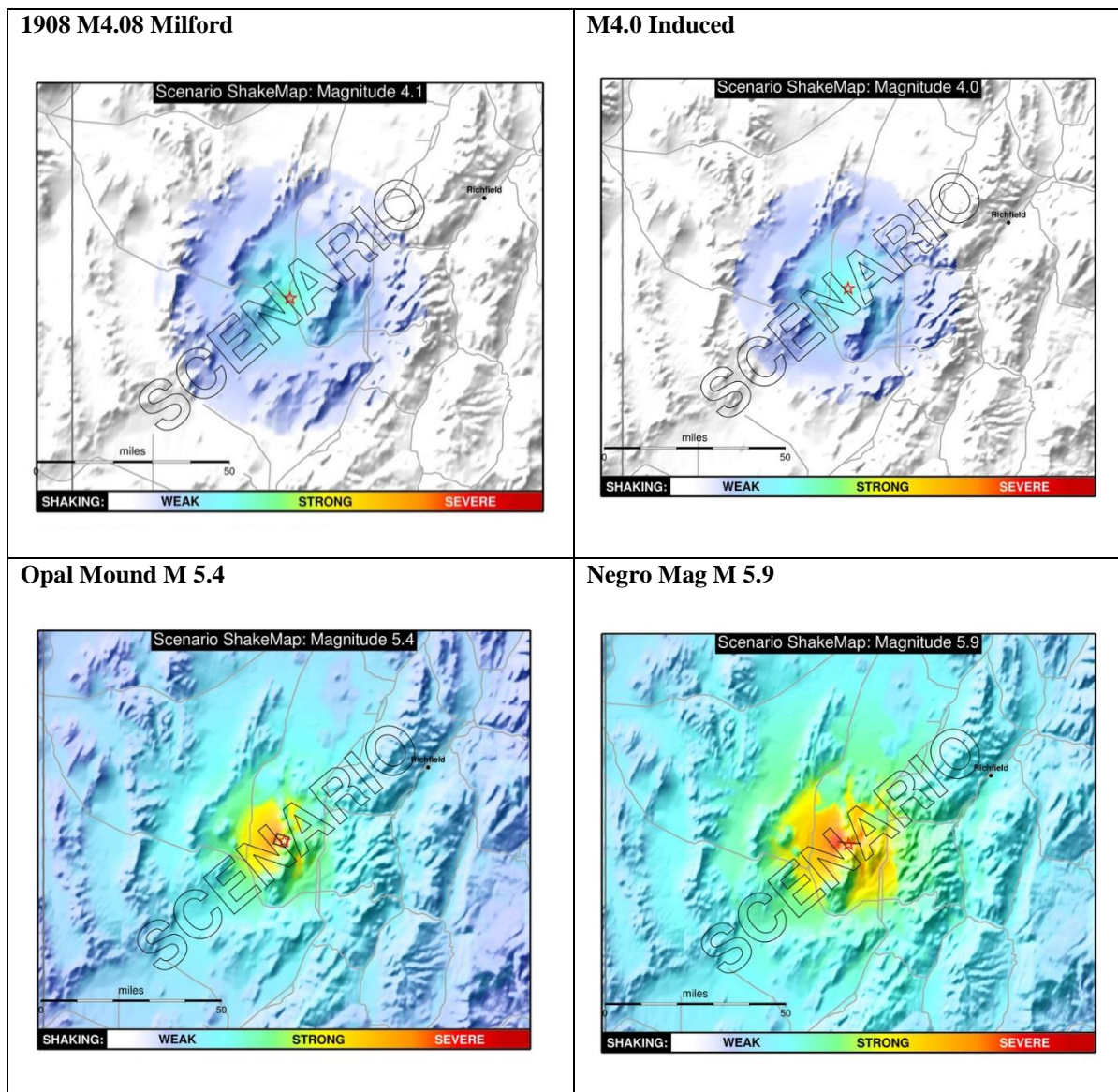


Figure 11. *Deterministic intensity maps for four potential scenario earthquakes near the Utah FORGE site. Maps were generated using ShakeMap (Wald et al., 1999; Worden and Wald, 2016). Maximum magnitude (ground motions) based on fault dimension (Table 1) for Opal Mound and Negro Mag scenarios (gray box surface projection of fault trace). Point sources assumed for Milford and potential induced earthquake*

For the two M 4 earthquakes, Induced and Milford, the maximum PGA is ~3%g at the epicenter, which based on ShakeMap relates to light perceived shaking and no potential for structural damage. The maximum PGA for the Opal Mound fault earthquake scenario is ~28%g over the rupture area (close to the Utah FORGE site) and falls off to ~10%g in Milford. Again, based on ShakeMap relations, this translates to the potential for moderate damage at the epicenter, but light potential damage in Milford. For the Negro Mag fault scenario, the PGA near the Utah FORGE site is ~35%g and for Milford and Beaver, the PGA is <10%g. For the area near the Utah FORGE site, potential damage could be moderate to moderate-heavy. Based on these

scenarios, potential damage to the nearby, populated centers is predicted to be light. The larger potential ground motions are located near the Utah FORGE site. Structures in the affected area include the well-site, wind mills related to the wind farm, and the Blundell Power Plant. As part of Phase 2 work, we will assess the potential vulnerability of these structures to the potential ground motions. For this work, we will need additional analysis of the spectral accelerations. The wind mills should be designed for large shear forces related to wind, but we will look into the resonance frequencies.

6. Risk of Induced Seismic Events

For the preliminary phase of this report, we have generated a HAZUS run based on the Opal Mound fault deterministic scenario (Figure 11). Based on fault proximity to the Utah FORGE site, we assume this scenario might represent the maximum earthquake for the area. Based on this initial HAZUS run, where we used the default HAZUS database, slight damage is predicted for < 5 residential structures and no damage is predicted for other building types, including schools and industry. There is no predicted damage to essential facilities such as hospitals, schools, police and fire stations, which are expected to have > 50% functionality on day 1. Overall HAZUS (with the default database) shows that the damage and loss from this earthquake is predicted to be minimal. Note that the default database does not include the wind farm or power plant. In Phase 2B, we will take a more detailed look at the inventory used for this run, in order to confirm these results. We will also add to the inventory the wind farm and the Blundell Power Plant, in order to predict any potential damage and loss to these facilities.

7. Risk-Based Mitigation Plan

This section of the report will be addressed in Phase 2B. After a more complete analysis with the new data.

Arabasz, W. J., Pechmann, J. C., and Burlacu, R., 2015, A uniform moment magnitude earthquake catalog for the Utah Region (1850–2012) and estimation of unbiased recurrence parameters for background seismicity [poster]: Proceedings Volume, Basin and Range Province Seismic Hazards Summit III, Utah Geological Survey Miscellaneous Publication 15-5 (CDROM).

Atkinson, G.M., and Boore, D. (2011) Modifications to existing ground-motion prediction equations in light of new data: Bull. Seism. Soc. Am., 101, 1121-1135.

Asanuma, H., Soma, N., Kaieda, H., Kumano, Y., Izumi, T., Tezuka, K., Niitsuma, H., and Wyborn, D. (2005) Microseismic monitoring of hydraulic stimulation at the Australian HDR project in Cooper Basin. In Proceedings World Geothermal Congress, 24-29.

Baisch, S., Weidler, R., Vörös, R., Wyborn, D., & de Graaf, L. (2006). Induced seismicity during the stimulation of a geothermal HFR reservoir in the Cooper Basin, Australia. Bulletin of the Seismological Society of America, 96(6), 2242-2256.

Benato, S., Reeves, D. M., Parashar, R., Davatzes, N. C., Hickman, S., Elsworth, D., Spielman, P., and Taron, J. (2013) Computational investigation of hydro-mechanical effects on transmissivity evolution during the initial injection phase at the Desert Peak EGS Project,

- NV. Proceedings, Thirty-Eighth Workshop on Geothermal Reservoir Engineering Stanford University, Stanford, California, February 11-13, 2013.
- Bradford, J., McLennan, Moore, J., Podgorney, R., Nash, G., Mann, M., Rickard, W., Glaspey, D. (2016). Numerical Modeling of the Stimulation Program at RRG-9 ST1, a DOE EGS. Proceedings, 41st Workshop on Geothermal Reservoir Engineering Stanford University, Stanford, California, Feb 22-24, 2016
- Breede, K., Dzebisashvili, K., Liu, X., and Falcon, G. (2013) A systematic review of enhanced (or engineered) geothermal systems: past, present and future. *Geothermal Energy*, 1, 4
- Bromley, C. J. and Majer, E. L. (2012) Geothermal induced seismicity - risks and rewards. New Zealand Geothermal Workshop 2012 Proceedings, 19-21 November, Auckland, New Zealand.
- Bommer, J.J., Oates, S., Cepeda, J.M., Lindholm, C., Bird, J., Torres, R., Marroquin, G., Rivas, J. (2006) Control of hazard due to seismicity induced by a hot fractured rock geothermal project. *Engineering Geology* 83, 287–306.
- Brown D (2009) Hot Dry Rock Geothermal Energy: important lessons from Fenton Hill. Paper presented at thirty-fourth workshop on geothermal reservoir engineering, Stanford University, Stanford, 9–11 Feb 2009
- Chabora, E., Zemach, E., Spielman, P., Drakos, P., Hickman, S., Lutz, S., Boyle, K., Falconer, A., Robertson-Tait, A., Davatzes, N. C., Rose, P., Majer, E., and Jarpe, S. (2012) Hydraulic stimulation of well 27-15, Desert Peak Geothermal Field, Nevada, USA. Proceedings, Thirty-Seventh Workshop on Geothermal Reservoir Engineering Stanford University, Stanford California, January 30- February 1, 2012.
- Cladouhos, T. T., Petty, S., Swyer, M. W., Uddenberg, M. E., and Nordin, Y. (2015) Results from Newberry Volcano EGS Demonstration. Proceedings, Fortieth Workshop on Geothermal Reservoir Engineering Stanford University, Stanford California, January 26-28.
- Chambers, D., K. D. Koper, K.L. Pankow, and M. K. McCarter (2015). Detecting and characterizing coal mine related seismicity in the Western U.S. using subspace methods, *Geophys. J. Intl.*, 203, 1388-1399.
- Chiou, B. and Youngs, R., 2008, An NGA model for the average horizontal component of peak ground motion and response spectra: *Earthquake Spectra*, v. 24, p. 173–216.
- Chiou, B., Youngs, R., Abrahamson, N., and Addo, K. (2010) Ground-motion attenuation model for small-to-moderate shallow crustal earthquakes in California and its implications for regionalization of ground-motion prediction models: *Earthquake Spectra*, v. 26, p. 907–926.
- Concha, D., Fehler, M., Zhang, H. and Wang, P. (2010) Imaging of the Soultz enhanced geothermal reservoir using microseismic data. Proceedings, thirty-fifth workshop on geothermal reservoir engineering Stanford University, Stanford, California, February 1-3.

- Cornet, F. H. and Burlet, D. (1992) Stress field determinations in France by hydraulic tests in boreholes. *Journal of Geophysical Research*, 97 (B8), 11829-11849.
- Correia, H., Sigurdsson, O., Sanjuan, B., Tulinius, H. and Lasne, E. (2000) Stimulation of a high-enthalpy geothermal well by cold water injection. *Geothermal Resources Council Transactions*, 24, Sep 24-27.
- Dallmeyer, R. D. and Liotta, D. (1998) Extension, uplift of rocks and cooling ages in thinned crustal provinces; the Larderello geothermal area (inner Northern Apennines, Italy). *Geological Magazine*, March 135, 193-202.
- Evans, K. F., Moriya, H., Niitsuma, H., Jones, R. H., Phillips, W. S., Genter, A., Sausse, J., Jung, R., and Baria, R. (2005) Microseismicity and permeability enhancement of hydrogeologic structures during massive fluid injections into granite at 3 km depth at the Soultz HDR site. *Geophysics Journal International* 160, 388-412.
- Evans, K. F., Zappone, A., Kraft, T., Deichmann, N. and Moia, F. (2012) A survey of the induced seismic responses to fluid injection in geothermal and CO₂ reservoirs in Europe. *Geothermics*, 41, 30-54.
- Garcia, J., Walters, M., Beall, J., Hartline, C., Pingol, A., Pistone, S., and Wright, M. (2012) Overview of the northwest geysers EGS demonstration project. *Proceedings, thirty-seventh workshop on geothermal reservoir engineering, Stanford University, Stanford California, January 30 - February 1, 2012.*
- Ghassemi, A., Alexis, D. A., Vardcharagossad, P., and Krishnamoorthy, V. (2010) Feasibility and Design of an Engineered Geothermal System using Dry and Abandoned Holes as a Prospective Location, Penn State.
- Gibowicz, S. J. (2009), Seismicity induced by mining: Recent research, *Adv. Geophys.*, 51, 1–53.
- Gischig, V. S. (2015), Rupture propagation behavior and the largest possible earthquake induced by fluid injection into deep reservoirs, *Geophys. Res. Lett.*, 42, 7420–7428, doi:10.1002/2015GL065072.
- Gregor, N., N. A. Abrahamson, G. M. Atkinson, D. M. Boore, Yo. Bozorgnia, K. W. Campbell, B. S.-J. Chiou, I. M. Idriss, R. Kamai, E. Seyhan, W. Silva, J. P. Stewart, and R. Youngs (2014) Comparison of NGA-West2 GMPEs. *Earthquake Spectra*: August 2014, Vol. 30, No. 3, pp. 1179-1197. doi: <http://dx.doi.org/10.1193/070113EQS186M>
- Haring, M. O., Schanz, U., Ladner, F., and Dyer, B. C., (2008) Characterization of the Basel 1 enhanced geothermal system. *Geothermics*, 37, 469-495.
- Healy, J.H., W.W. Rubey, D.t. Griggs, and C.B. Raleigh (1968) The Denver earthquakes, *Science*, 161, 1301-1310.
- Jones, C., Moore, J., Teplow, W., and Craig, S. (2011) Geology and hydrothermal alteration of the Raft River geothermal system, Idaho. *Proceedings, thirty-sixth workshop on*

geothermal reservoir engineering Stanford University, Stanford, California, January 31 - February 2, 2011.

- Julian, B. R., Foulger, G. R., and Monastero, F. C. (2009) Seismic monitoring of EGS stimulation tests at the Coso geothermal field, California, using microearthquake locations and moment tensors. Proceedings, thirty-fourth workshop on geothermal reservoir engineering Stanford University, Stanford, California, February 9-11, 2009.
- Jung, R. (1989) Hydraulic In Situ Investigations of an Artificial Fracture in the Falkenberg Granite. *International Journal of Rock Mechanics and Mining Sciences & Geomechanics*, 26 (3/4), 301-308.
- Kaieda, H., Ito, H., Kiho, K., Suzuki, K., Suenaga, H., and Shin, K. (2005) Review of the Ogachi HDR Project in Japan. Proceedings World Geothermal Congress, Antalya Turkey, 24-29 April, 2005.
- Kaieda, H. (2014) Hijiori HDR Reservoir Evaluation by Micro-Earthquake Observation. *GRC Transactions*, Vol. 38.
- Kiraly, E., Gischig, V., Karvounis, D., and Wiemer, S. (2014) Validating Models to Forecasting Induced Seismicity Related to Deep Geothermal Energy Projects. Proceedings Thirty-Ninth Workshop on Geothermal Reservoir Engineering Stanford University, Stanford, California, February 24-26, 2014.
- Kolditz, O. and Clauser, C. (1998) Numerical simulation of flow and heat transfer in fractured crystalline rocks: application to the hot dry rock site in Rosemanow (U.KI.). *Geothermics*, 27 (1), 1-23.
- Kwiatek, G., Bohnhoff, M., Dresen, G., Schulze, A., Schulte, T., Zimmermann, G., and Huenges, E. (2010) Microseismicity induced during fluid-injection: a case study from the geothermal site at Groß Schönebeck, North German Basin. *Acta Geophysics*, 58, 995-1020.
- Kwiatek, G., Bulut, F., Bohnhoff, M., and Dresen, G. (2014) High-resolution analysis of seismicity induced at Berlin geothermal field, El Salvador. *Geothermics*, 52, 98-111.
- Majer, E. L., Bara, R., Stark, M., Oates, S., Bommer, J., Smith, B., and Asanuma, H. (2007) Induced seismicity associated with Enhanced Geothermal Systems. *Geothermics*, 36, 185-222.
- Majer, E., J. Nelson, A. Robertson-Tai, J. Savy, and I. Wong (2011), Protocol for addressing induced seismicity associated with Enhanced Geothermal Systems.
<<http://www1.eere.energy.gov/geothermal/pdfs/egs-is-protocol-final-draft-20110531.pdf>>.
- McDonald, G.N., and Ashland, F.X., 2008, Earthquake site conditions in the Wasatch Front urban corridor, Utah: Utah Geological Special Study 125, 41 p., 1 plate, scale 1:150,000, compact disk.
- McGarr, A. (1976), Seismic moments and volume changes, *J. Geophys. Res.*, 81, 1487-1494.

- McGarr, A. (2014), Maximum magnitude earthquakes induced by fluid injection, *J. Geophys. Res. Solid Earth*, 119, 1008–1019, doi:10.1002/ 2013JB010597.
- Meixner, J., Schill, E., Gaucher, E. and Kohl, T. (2014) Inferring the in situ stress regime in deep sediments: an example from the Bruchsal geothermal site. *Geothermal Energy*, 2 (7).
- Moeck, I., Bloch, T., Graf, R., Heuberger, S., Kuhn, P., Naef, H., Sonderegger, M., Uhlig, S., and Wolfgramm, M. (2015) The St. Gallen Project: Development of Fault Controlled Geothermal Systems in Urban Areas. *Proceedings World Geothermal Congress*, Melbourne, Australia, 19-25 April 2015.
- Oppenheimer, D. H. (1986) Extensional tectonics at The Geysers geothermal area, California. *Journal of Geophysical Research*, 91 (B11), 11463-11476.
- Osborn, W. L., Petty, S., Cladouhos, T. T., Lovenitti, J., Nofziger, L., Callahan, O., Perry, D., S., and Stern, P. S. (2011) Newberry Volcano EGS Demonstration-Phase 1 results. *GRC Transactions*, 35.
- Pankow, K. L., W. J. Arabasz, S. J. Nava, and J. C. Pechmann (2004). Triggered seismicity in Utah from the 3 November 2002 Denali fault earthquake, *Bull. Seism. Soc. Am.* 94, S332-S347.
- Petersen, Mark D., Frankel, Arthur D., Harmsen, Stephen C., Mueller, Charles S., Haller, Kathleen M., Wheeler, Russell L., Wesson, Robert L., Zeng, Yuehua, Boyd, Oliver S., Perkins, David M., Luco, Nicolas, Field, Edward H., Wills, Chris J., and Rukstales, Kenneth S., 2008, Documentation for the 2008 Update of the United States National Seismic Hazard Maps: U.S. Geological Survey Open-File Report 2008–1128, 61 p.
- Rutqvist, J., Jeanne, P., Dobson, P., Garcia, J., Hartline, C., Hutchings, L., Singh, A., Vasco, D., and Walters, M. (2015) The Northwest Geysers EGS Demonstration Project, California - Part 2: Modeling and interpretation. *Geothermics*, 2 Sep.
- Sasaki, S. and Kaieda, H. (2000) Determination of stress state at the Hijiori HDR site from focal mechanisms. *Proceedings of World Geothermal Congress*, 2000, 3859-3864.
- Schindler, M., Baumgartner, J., Gandy, T., Hauffe, P., Hettkamp, T., Menzel, H., Penzkofer, P., Teza, D., Tischner, T., and Wahl, G. (2010) Successful Hydraulic Stimulation Techniques for Electric Power Production in the Upper Rhine Graben, Central Europe. *Proceedings World Geothermal Congress 2010*, Bali Indonesian, April 25-29.
- Shapiro, S. A., O. S. Kruger, C. Dinske, and C. Langenbruch (2011), Magnitudes of induced earthquakes and geometric scales of fluid- stimulated rock volumes, *Geophysics*, 76, WC55–WC63, doi:10.1190/GEO2010-0349.1
- Simpson, D. W., W.S. Leith, and C.H. Scholz (1988) Two types of reservoir-induced seismicity, *Bull. Seism. Am.*, 78, 2025-2040.
- Tenzer, H., Schanz, U., Stang, H., Baisch, S., and Weidler, R. (2004) Potential for geothermal power production from deep hot crystalline rock at Bad Urach (southern Germany). *Zeitschrift fuer Angewandte Geologie*, 50 (2), 43-49.

- Tester, J. W., Anderson, B. J., Batchelor, A. S., Blackwell, D. D., DiPippo, R., Drake, E. M., Garnish, J., Livesay, B., Moore, M.C., Nichols, K. and Petty, S. (2006). The future of geothermal energy. Impact of Enhanced Geothermal Systems (EGS) on the United States in the 21st Century, Massachusetts Institute of Technology, Cambridge, MA, 372.
- Torio-Henríquez, E. (2007) Petrography and mineral alteration in Berline geothermal field. Proceedings of the thirty-second workshop on geothermal reservoir engineering Stanford University, Stanford California, January 22-24, 2007.
- Traineau, H., Beaufort, D., Brach, M., Castaing, C., Genter, A. and Herbrich, B. (1997) The Bouillante geothermal field (F.W.I.) revisited: new data on the fractured-geothermal reservoir in light of a future stimulation experiment in a low productive well. Proceedings, twenty-second workshop on geothermal reservoir engineering Stanford University, Stanford, California, January 27-29, 1997.
- Wald, David J., Vincent. Quitoriano, Tom. H. Heaton, Hiroo. Kanamori, Craig. W. Scrivner, and C. Bruce Worden, (1999). TriNet ``ShakeMaps'': Rapid Generation of Instrumental Ground Motion and Intensity Maps for Earthquakes in Southern California Earthquake Spectra, 15, 537-556
- Wald, D. J., C. B. Worden, V. Quitoriano, and K.L. Pankow (2005) ShakeMap Manual: Users Guide, Technical Manual, and Software Guide: U.S. Geological Survey Techniques and Methods 12-A1, 128pp.
- Walter, A. W. and Weaver, C. (1980) Seismicity of the Coso Range, California. Journal of Geophysical Research, 85 (B5), 2441-2458.
- Wang, R., Y.J. Gu, R. Schultz, A. Kim, and G. Atkinson (2016) Source analysis of a potential hydraulic-fracturing-induced earthquake near Fox Creek, Alberta, Geophys. Res. Lett., 43, 564-573, DOI: 10.1002/2015GL066917
- Wells, D. L. and K. J. Coppersmith (1994). New empirical relationships among magnitude, rupture length, rupture width, rupture area, and surface displacement, Bull. Seism. Soc. Am. 84, 974,1002.
- Williams, P. L., Covington, H. R., and Pierce, K. L. (1982) Cenozoic stratigraphy and tectonic evolution of the Raft Tier Basin, Idaho: Cenozoic geology of Idaho, Idaho Bureau of Mines and Geology Bulletin 26, 491-504.
- Worden, C. B., and D. J. Wald (2016). ShakeMap Manual, February 01, 2016. <http://dx.doi.org/10.5066/F7D21VPQ>
- Wyborn, D., de Graaf, L., and Hann, S. (2005) Enhanced geothermal development in the Cooper Basin, South Australia. Geothermal Resources Council Transactions, 151-156.
- Zang, A., Oye, V., Jousser, P., Deichmann, N., Gritto, R., McGarr, A., Ernest, M. and Bruhn, D. (2014) Analysis of induced seismicity in geothermal reservoirs-An overview. Geothermics, 52, 6-21.

Zandt, G., L. McPherson, S. Schaff and S. Olsen, Seismic baseline and induction studies: Roosevelt Hot Springs, Utah, and Raft River, Idaho, U.S. Dept of Energy rept. DOE/ID/01821-T1, 58 pp., 1982.